JOURNAL OF VIROLOGY, Feb. 2007, p. 1879–1887 Vol. 81, No. 4
0022-538X/07/$08.00+0 doi:10.1128/JVI.01899-06

Deterministic, Compensatory Mutational Events in the Capsid of Foot-and-Mouth Disease Virus in Response to the Introduction of Mutations Found in Viruses from Persistent Infections▽

Roberto Mateo and Mauricio G. Mateu*

Centro de Biología Molecular Severo Ochoa (CSIC-UAM), Universidad Autónoma de Madrid, Cantoblanco, 28049 Madrid, Spain

Received 31 August 2006/Accepted 23 November 2006

The evolution of foot-and-mouth disease virus (FMDV) (biological clone C-S8c1) in persistently infected cells led to the emergence of a variant (R100) that displayed increased virulence, reduced stability, and other modified phenotypic traits. Some mutations fixed in the R100 genome involved a cluster of highly conserved residues around the capsid pores that participate in interactions with each other and/or between capsid protomers. We have investigated phenotypic and genotypic changes that occurred when these replacements were introduced into the C-S8c1 capsid. The C3007V and M3014L mutations exerted no effect on plaque size or viral yield during lytic infections, or on virion stability, but led to a reduction in biological fitness; the D3009A mutation caused drastic reductions in plaque size and viability. Remarkably, competition of the C3007V mutant with the nonmutated virus invariably resulted in the fixation of the D3009A mutation in the C3007V capsid. In turn, the presence of the D3009A mutation invariably led to the fixation of the M3014L mutation. In both cases, two individually disadvantageous mutations led, together, to an increase in fitness, as the double mutants outcompeted the nonmutated genotype. The higher fitness of C3007V/D3009A was related to a faster multiplication rate. These observations provide evidence for a chain of linked, compensatory mutational events in a defined region of the FMDV capsid. Furthermore, they indicate that the clustering of unique amino acid replacements in viruses from persistent infections may also occur in cytolytic infections in response to changes caused by previous mutations without an involvement of the new mutations in the adaptation to a different environment.

Biologically disadvantageous mutations can be fixed in a genome if second-site, compensatory mutations that are able to restore the biological fitness are also fixed before the primary mutation leads to extinction of the mutated genome. Partially or fully compensatory mutations in proteins from cellular organisms or viruses may be a frequent occurrence in nature, as indicated by both theoretical (see, e.g., references 30 and 31) and experimental (see, e.g., references 10, 11, 15, 26, 36, 38–45, 52, 53, 58, and 59) analyses. Intramolecular compensatory mutations in proteins can sometimes occur in residues located far away from the primary mutation but appear to have a tendency to involve spatially close residues (23, 33, 56, 57). In a few cases, detailed structure-function studies have provided some insight into the molecular mechanisms of compensatory effects (5, 6, 7, 12, 21, 27–29, 37). The bases of the compensatory effects range from near-additive, nonspecific (global) effects on a single property of the protein, such as stability, to complex, nonadditive, multifactorial effects including altered interaction patterns and propagated conformational rearrangements. However, for the large majority of compensatory effects detected, the mechanistic explanation remains unclear. In addition to intrinsically advantageous second-site mutations acting merely in an additive way with the disadvantageous primary mutation, intrinsically near-neutral compensatory mutations have been observed in some cases (46, 48). Mutually compensatory effects of individually disadvantageous mutations leading to a neutral phenotype, or even providing a selective advantage relative to the situation where no mutation is present, may also occur in proteins (3, 25, 36). However, these effects have been much less documented so far.

The rapid replication, high mutation rates, and large population sizes of RNA viruses lead to genetically highly heterogeneous populations, termed viral quasispecies (for some reviews, see references 17, 18, 19, and 20). Viral quasispecies have an enormous potential for rapid evolution through adaptation to new environments. As quasispecies contain not only many different single mutants but also many different multiple mutants, evolution through the simultaneous or sequentially rapid fixation of combinations of mutations, including compensatory mutations, may occur very frequently in RNA viruses. Indeed, many documented cases of compensatory mutations (see references mentioned above) involve proteins from RNA viruses.

The establishment and maintenance of a persistent infection of mammalian cells by a picornavirus, foot-and-mouth disease virus (FMDV), involved the coevolution of cells and virus (13, 14). The determinant element in the initiation of the persistent infection was the selection of cell variants with a slightly increased resistance to the FMDV clone (C-S8c1) used to initiate the infection (34). The surviving cells became increasingly resistant to infection, while the virus shed evolved to become

* Corresponding author. Mailing address: Centro de Biología Molecular Severo Ochoa, Universidad Autónoma de Madrid, Cantoblanco, 28049 Madrid, Spain. Phone: 34-91-4978462. Fax: 34-91-4974799. E-mail: mgarcia@cbm.uam.es.

▽ Published ahead of print on 6 December 2006.

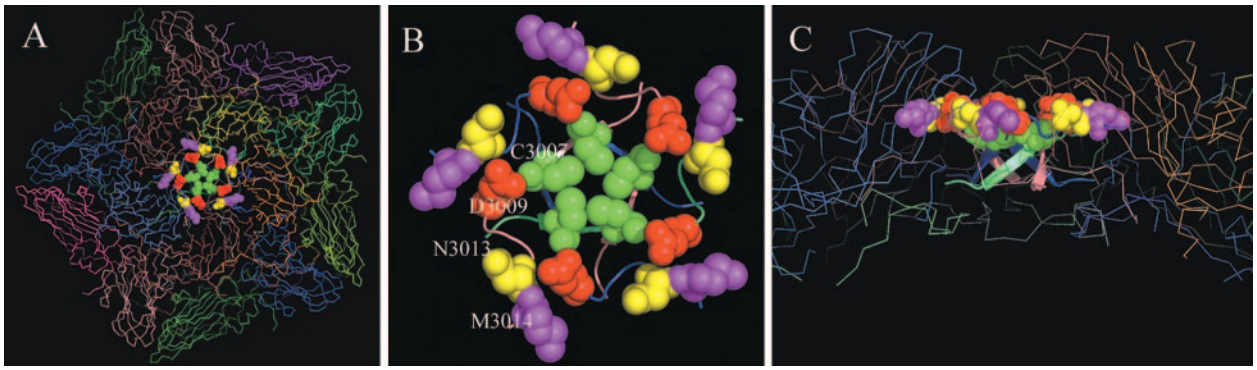

FIG. 1. Location in the virus capsid of a cluster of residues found to be mutated in FMDV R100. (A) Cα tracing model of a pentameric subunit in the FMDV C-S8c1 capsid viewed from the exterior of the virion. Five copies of each of the capsid proteins VP1, VP2, VP3, and VP4 are depicted in different colors. The residues around the fivefold axis pore (center) that were found to be mutated in FMDV R100 (16) are represented as space-filling models and are color coded (green, Cys3007; red, Asp3009; yellow, Asn3013; magenta, Met3014). (B) Close-up view of the N termini of five symmetry-related copies of VP3 around the fivefold axis pore in a pentamer shown in the same orientation depicted in A. The tracing of the main-chain backbone is indicated by ribbons. The residues that were found to be mutated in FMDV R100 are represented as in A. The five cysteine residues (green) constrict the pore (center). (C). Side view of the fivefold axis region in a pentamer. The outer surface is up. The β-annulus formed by β-strands belonging to the five VP3 subunits (colored arrows) is shown below the residues found mutated in FMDV R100 (shown as colored space-filling models as in A and B).

progressively more virulent to the original cells and acquired, in addition, other phenotypic traits. These traits included a smaller plaque size, temperature sensitivity, and a reduced stability of the virion during purification (13, 16, 49). Nucleotide sequencing revealed that several mutations had been fixed in the C-S8c1 genome during the persistent infection (16, 54). In particular, nine amino acid substitutions were identified in the capsid of the virus (R100) rescued after 100 passages of persistently infected cells (16). Most of these substitutions had not occurred in previously sequenced FMDV variants, which were generally isolated from animals acutely infected in the field or from cytolytic infections in the laboratory, or even in related picornaviruses. These results led those authors to conclude that if provided with a new suitable environment, like residence in carrier cells, even positions in the viral genome that are regarded as highly invariant can be subjected to rapid change (16).

A major interest of our group is the study of the molecular determinants of assembly and stability of viruses. In a previous analysis, we provided evidence that in FMDV, most residues at the capsid interpentamer interfaces, and their interactions, are important for the infectivity, and stability, of the virion (35). In addition, a few mutations outside these interfaces have been shown to have an effect on the conformational stability of picornaviruses, including FMDV (2, 24, 50, 55). Four (nearly half) of the mutations in the capsid of FMDV R100 involve identical clusters of residues that surround the pores at each capsid fivefold symmetry axis (16) (Fig. 1) and are also a part of the interfaces between the capsid protomers. The low stability of R100 during purification, and its temperature sensitivity in cytolytic infections, led us to investigate whether this cluster of mutations in the R100 capsid and, specifically, the loss of interprotomer disulfide bonds and salt bridges around those pores (because of C3007V and D3009A mutations) could be responsible for a low conformational stability. We were also interested in determining whether these clustered mutations could act through nonadditive ("epistatic") and perhaps compensatory effects. The mutations have been introduced into an infectious FMDV clone, and their effects on infectivity and particle stability and on the biological fitness of the virus in competition experiments have been analyzed. We have found unexpected, complex mutation dynamics that involved the repeated fixation in a cytolytic infection context of some of the mutations previously found in R100, a virus that emerged in a persistent infection context. In addition, combinations of these mutations led to complex compensatory effects and an increase in the biological fitness of cytolytic infections.

MATERIALS AND METHODS

Viruses and plasmids. FMDV C-S8c1 is a plaque-purified derivative of serotype C isolate C_1Santa Pau-Sp70 (51). Plasmids pO_1K/C-S8c1 and p3242/C-S8c1 have been described previously (4). pO_1K/C-S8c1 was derived from an infectious cDNA clone obtained by Zibert and coworkers (60) from FMDV O_1Kaufbeuren. pO_1K/C-S8c1 contains a cDNA copy of an infectious chimeric FMDV genome coding for the capsid proteins and protease 2A of C-S8c1, a chimeric 2B protein, and all other nonstructural proteins of O_1Kaufbeuren. Plasmid p3242/C-S8c1 contains a segment of 3,242 bp (between the two NgoMIV sites in the pO_1K/C-S8c1 plasmid that includes the entire capsid region coding for the capsid proteins of FMDV C-S8c1) inserted into a vector derived from plasmid pGEM-5Zf(+) (4). Plasmid $pO_1K/\Delta 2292$ corresponds to pO_1K/C-S8c1 with a segment of 2,292 bp (between the AflII and AvrII restriction sites) deleted. This segment includes part of the L protease and the entire capsid region coding for the capsid proteins, except for a short C-terminal segment of VP1 (identical in sequence between C-S8c1 and O_1K).

Site-directed mutagenesis, subcloning, and DNA sequencing. Site-directed mutagenesis of FMDV capsid residues was carried out on plasmid p3242/C-S8c1 by an inverse PCR method using the QuikChange site-directed mutagenesis kit (Stratagene). The mutations introduced were confirmed by automated sequencing using dideoxynucleotide terminators. The sequences were obtained by the Genomic Unit of the Madrid Science Park at the Universidad Autónoma de Madrid. The ABI PRISM BigDye Terminator kit and an ABI PRISM 3730 or ABI PRISM 3700 automated sequencer (Applied Biosystems) were used. A region of about 600 nucleotides around the introduced mutations was sequenced in each case. For some mutants, indicated in Results, the entire sequence of the 2,292-bp segment to be subcloned was determined. No second-site mutations were found in the mutated plasmid. The mutagenized 2,292-bp segments were subcloned into $pO_1K/\Delta 2292$ to obtain pO_1K/C-S8c1 plasmids, and the presence of the introduced mutation was again checked by sequencing.

Transcription of viral RNA and electroporation of eukaryotic cells. Transcription and transfection of infectious viral RNA have been previously described (35). In each experiment, the same amount of mutated and nonmutated FMDV RNA was used. A negative control containing no viral RNA was also included.

Titration, amplification of viruses, and extraction of viral RNA. Virus titers were always determined at least in duplicate in standard plaque assays. When necessary, mutant virions obtained were amplified by a single passage in BHK-21 cell monolayers at the highest possible multiplicity of infection (MOI). Extraction of viral RNA was performed by using TRIzol (Invitrogen) essentially as described previously (35).

Competition assays. Confluent BHK-21 cell monolayers cultured in B25 flasks (3×10^6 cells) were infected with a mixture containing equal amounts of the competing viruses at an MOI of 0.1. Adsorption of viruses was allowed to proceed for 60 min at 37°C. Fresh Dulbecco's modified Eagle medium (DMEM) supplemented with 2% fetal calf serum was then added. Viruses were harvested when a complete cytopathic effect was observed, clarified by centrifugation, and diluted 10 times with fresh DMEM. A fraction of the supernatant was stored at −70°C and used for RNA extraction. Another fraction of the supernatant was used to infect new cell monolayers. This cycle of infection and harvest was repeated up to seven times. For each pair of competing viruses, the experiment was independently repeated two or three times. When eight passages had been completed, the RNA of the viral populations obtained at different passages was extracted, reverse transcribed and amplified by reverse transcription-PCR, and sequenced as described above to estimate the degree of dominance of each of the two competing viruses at the passage considered and whether other mutations had been fixed in a detectable proportion of the viral RNA molecules during replication. In general, the entire capsid-coding region was sequenced. In some cases, as indicated in Results, the entire genome was sequenced. The approximate proportions of the competing genomes and of any other mutation that happened to arise during replication were estimated by densitometry of the chromatogram peaks corresponding to the nucleotide present in the mutant virus and the nucleotide present in the nonmutated virus. The ratio of the integrated areas under each peak was used to estimate the ratio of mutant genomes to nonmutant genomes at the position considered.

Kinetic assays of virus production. For each assay, two confluent BHK-21 cell monolayers in P60 petri dishes (2.5×10^6 cells) were infected with the chosen mutant FMDV or with FMDV C-S8c1 at an MOI of 10. The progression of the cytopathic effect was compared at different times by examination under a microscope. The kinetics of extracellular viral production were determined by the titration of aliquots taken at different times postinfection. Production assays were always carried out in duplicate. For each assay, titers were also always calculated in duplicate.

Thermal inactivation assays. Two types of assays were used. In the first type, 1-ml aliquots of cell culture supernatants obtained from cytolytic infections or after viral RNA transfection of cell monolayers containing viral populations with an approximate titer of 2×10^7 to 4×10^7 PFU/ml were clarified and subsequently heated for different lengths of time at 42°C. The percentage of infectious particles remaining after heating was determined by use of standard plaque assays, and the values obtained at different times were fitted to a first-order exponential decay model by using the program Kaleidagraph (Abelbeck Software) to obtain the inactivation rate constant (35). Alternatively, the logarithmic values of the viral titers were linearly fitted using the same program. In a second type of assay, the same cell culture supernatants containing virus populations were diluted in DMEM plus 2% fetal calf serum to a final concentration of about 1,000 PFU/ml. Aliquots (100 μl) of the diluted samples were incubated for different lengths of time at 42°C, and the percentage of infectious particles remaining after heating was determined by plaque assays as described above.

RESULTS

Effect of mutations around the fivefold axes of the R100 capsid on FMDV infectivity. Four of the capsid residues of FMDV C-S8c1 that were found to be mutated in FMDV R100 (Cys3007, Asp3009, Asn3013, and Met3014) are located very close or in contact to each other, in the vicinity of the pores at each capsid fivefold axis (16) (Fig. 1). In FMDV, this is the region where multiple interactions between the five protomer subunits that form each pentamer occur. These interactions include interchain hydrogen bonds between the N terminus of five symmetry-related VP3 subunits to form a parallel β-annulus (1, 32) (Fig. 1B and 1C). In FMDV C-S8c1 (32) as well as in other variants (1), the side chains of Cys3007 belonging to the five symmetry-related VP3 subunits protrude inwards from the β-annulus and constrict the fivefold axis (Fig. 1B). Electrophoretic analyses of both C-S8c1 (16) and a mutant in which Cys3007 was replaced by Val (data not shown), under reducing and nonreducing conditions, revealed that the Cys3007 side chains participate in up to two disulfide bonds between four of the five neighboring protomers surrounding each fivefold axis pore. In the crystallographic models of FMDV (1, 32), the five cysteines appear to be symmetrically arranged, but this is almost certainly the result of symmetry averaging during the generation of the models. The side chain of Asp3009 in each protomer is also involved in interprotomer interactions, participating in salt bridges with Lys1109 of VP1 from a different protomer; in addition, the side chains of Asn3013 and Met3014 participate in intraprotomer van der Waals interactions between them (1, 32). The R100 mutations (C3007V, D3009A, N3013H, and M3014L) disrupted the disulfide bonds, salt bridges, and most other interactions of the original residues and substantially altered the stereochemistry and chemical character of an annulus of residues surrounding each capsid pore (Fig. 1).

Analyses of 211 FMDV sequences currently available from the GenBank database confirmed a previously reported observation (16) that Asp3009 is highly conserved (98%) in FMDV from acute/lytic infections and that Cys3007 is also remarkably conserved (87%). To determine whether mutations of residues Cys3007 or Asp3009 and the respective removal of disulfide bonds or buried salt bridges had an effect on the infectivity and/or stability of FMDV, we introduced them individually into the capsid of C-S8c1, the virus used to establish a persistent infection. Viral RNAs carrying the C3007V or D3009A mutation and nonmutated viral RNA were obtained from an infectious DNA clone with the corresponding mutation and were used to electroporate susceptible cells. The progeny virus populations obtained were collected and titrated (Table 1). Relative to the nonmutated control, no significant differences in viral titer at 45 h or 55 h postelectroporation, or in plaque size, were observed for the C3007V mutant in repeated electroporation assays. In contrast, for the D3009A mutant, nine independent electroporations yielded widely different virus titers at 45 h postelectroporation, with values that ranged from undetectable to a titer close to that of the nonmutated control. On most occasions, plaque size heterogeneity was also observed. In one experiment, D3009A populations were recovered at 45 h, 55 h, and 95 h postelectroporation, and a gradual increase in titer, up to nearly wild-type levels, was observed (Table 1). These data suggested that the D3009A mutation had a drastic negative effect on infectivity and that reversion or new mutations had occasionally occurred during the replication of D3009A, leading to heterogeneous populations with variable amounts of virus genotypes that differed drastically in infectivity.

To ascertain if the introduced mutations were still present in the progeny viruses, and whether other mutations had been fixed after electroporation, the total RNA extracted from the virions in the populations obtained with either C3007V or D3009A was sequenced. For C3007V, it was found that the original mutation was still present in all nine populations ob-

TABLE 1. Values of viral titer and plaque size for a set of viruses with mutations around the fivefold axis of the FMDV capsid

Electroporated viral RNA	Virus titer[a] (PFU/ml)			Global sequence (% of molecules)[b]	Plaque size[c]
	45 h p.t.	55 h p.t.	95 h p.t.		
Parental	2.6×10^6	2.6×10^6	1.9×10^6	No mutations	Large
C3007V (9 expts)	3.13×10^6	6.3×10^5	3×10^3	C3007V (100)	Large
D3009A (expt a)	<50	ND	ND	NA	NA
D3009A (expt b)	<50	ND	ND	NA	NA
D3009A (expt c)	<50	ND	ND	NA	NA
D3009A (expt d)	3×10^2	ND	ND	NA	Small
D3009A (expt e)	3.5×10^3	4.1×10^4	1.1×10^5	D3009A (100) + M3014L (40)	Heterogeneous
D3009A (expt f)	2.5×10^5	ND	ND	D3009A (100) + M3014L (60)	Heterogeneous
D3009A (expt g)	3.1×10^5	ND	ND	D3009A (100) + M3014L (60)	Heterogeneous
D3009A (expt h)	3.3×10^5	ND	ND	D3009A (100) + M3014L (70)	Heterogeneous
D3009A (expt i)	1×10^6	ND	ND	D3009A (100) + M3014L (70)	Heterogeneous
M3014L (1 expt)	1.9×10^6	2.1×10^6	3.5×10^6	M3014L (100)	Large
D3009A/M3014L (1 expt)	2.8×10^5	1.7×10^6	1.6×10^6	D3009A (100) + M3014L (100); D3009A (100) + M3014L (100) + N3013H (50) at 95 h p.t.	Large

[a] BHK cells were electroporated with nonmutated or mutant viral RNA as described in Materials and Methods. As a measure of the reproducibility of both transfection and titration experiments, the parental (control) RNA was independently transfected nine times, yielding very similar results in all cases. The average titer of the progeny populations is indicated. ND, not determined. Every transfection experiment with mutants included a parallel transfection with the nonmutated control, which was also titrated, as an internal positive control of the viral yield. Virus titers are given at the indicated times (hours) posttransfection (p.t.). For the D3009A mutant, the viral yield and global sequence heterogeneity differed widely in nine independent experiments (see the text) and are indicated separately. These experiments are listed according to increasing values for the virus titer obtained at 45 h p.t. (experiments a to i).

[b] Total RNA from each viral progeny at 45 h p.t. was obtained as described in Materials and Methods. For each population, the mutations found relative to C-S8c1 are indicated, and the approximate percentage of molecules carrying the mutation are given in parenthesis (see the text). For the C3007V mutant, the entire genome sequence was determined. For all other mutants, the sequence of the complete capsid region (P1) was determined. NA, not applicable.

[c] Viruses that yielded plaques with sizes of 3 to 5 mm under the conditions of the assay were considered to have a large-plaque phenotype. All the other plaques with a lower diameter were considered small. *Heterogeneous* refers to a mixture of large-plaque and small-plaque phenotypes. NA, not applicable.

tained at 45 h postelectroporation. In one case, the entire genome was sequenced, which showed that no other mutation (either missense or silent) had been fixed in the C3007V population. For the D3009A mutation, the entire capsid region of the progeny viruses that were obtained in five out of the nine different experiments was sequenced. In experiment e (Table 1), the D3009A mutation was still dominant in the low-titer population obtained at 45 h postelectroporation, while reversion to Asp at position 3009 was dominant in the population obtained at 95 h, which approached the titer of the nonmutated control. Remarkably, in all five populations obtained at 45 h postelectroporation, Ala was still dominant at position 3009, but a mixture of Met and Leu in variable proportions was found at position 3014, spatially very close to residue 3009. When Met dominated at position 3014, the viral yield at 45 h postelectroporation was extremely low; when Leu dominated at the same position, the viral yield was orders of magnitude higher (Table 1). This latter result led us to introduce the M3014L single mutation and the D3009A/M3014L double mutation into the FMDV infectious clone to compare the individual and combined effects of these mutations in a genetically homogeneous background. Both the single mutant and the double mutant showed normal plaque sizes and yielded virus titers that approached that of the nonmutated control (Table 1). Sequencing of the entire capsid region of the populations obtained at 45 h postelectroporation showed that the introduced mutations were still present in the progeny viruses and that no other mutations had occurred. These and the above-mentioned results indicate that the D3009A mutant has drastically reduced infectivity in a cytolytic infection and that the infectivity can be recovered in the absence of reversion through the fixation of a second mutation, M3014L, in a neighboring capsid residue. Interestingly, the M3014L mutation had also occurred in FMDV R100 in addition to C3007V and D3009A. It is also worth noting that a new mutation, N3013H, was partially fixed in the D3009A/M3014L population recovered at 95 h postelectroporation. Again, this mutation had also been found in FMDV R100 in addition to C3007V, D3009A, and M3014L (16) (Fig. 1).

To summarize the above-described results, of the mutations that were fixed around the fivefold axes in the capsid of FMDV R100 during a persistent infection, C3007V and M3014L were individually tolerated without any substantial effect on the viral yield in cytolytic infections. In contrast, D3009A had a drastic negative effect on viability but strongly favored the fixation of the M3014L mutation at a neighboring position, leading to a compensatory effect that allowed the recovery of infectious virions in high yields. In turn, the D3009A/M3014L double mutation facilitated the partial fixation of the N3013H mutation, again at a neighboring position.

Effect of mutations around the fivefold axes of the R100 capsid on the thermostability of the FMDV virion. The thermostabilities of the viable C3007V mutants were determined in heat inactivation assays (Fig. 2). The inactivation rate constants at 42°C (average ± standard deviation of two or three determinations from independent experiments) were, respectively, 0.023 ± 0.010 min^{-1}, 0.013 ± 0.001 min^{-1}, and 0.023 ± 0.04 min^{-1}. By comparison, the inactivation rate constant of the nonmutated virus (obtained from 55 independent determinations as a measure of the reproducibility of the assay) was 0.019 ± 0.006 min^{-1}. In the case of the C3007V mutant and the nonmutated control, inactivation analyses of diluted or undiluted virus were carried out and yielded similar results (Fig. 2A and B, respectively). No substantial differences in thermostabilities were found between any of those three mutants and the nonmutated infectious virion (Fig. 2B). These

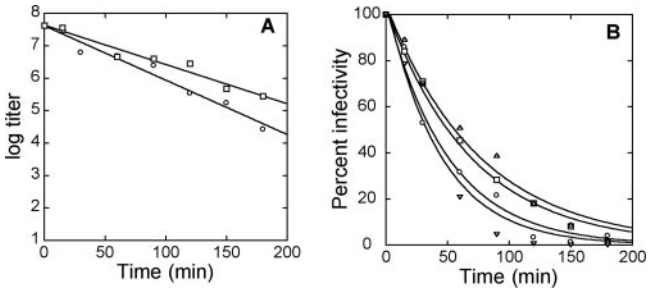

FIG. 2. Thermal inactivation kinetics of the parental and mutant FMDVs. (A) Inactivation of undiluted parental virus (circles) and mutant C3007V (squares) (using the first type of inactivation assay described in Materials and Methods) at 42°C. Linear fitting of the logarithmic values is indicated. (B) Inactivation of the diluted parental virus (circles), C3007V (squares), M3014L (triangles), and D3009A/M3014L (inverted triangles) (using the second type of inactivation assay described in Materials and Methods) at 42°C. Fitting of the data to a single exponential is indicated.

results reveal that contrary to what we suspected, Cys3007 and Met3014 alone or in combination with Asp3009 are not involved in the stabilization of the FMDV particle against thermal inactivation.

Effect of mutations around the fivefold axes of the R100 capsid on the biological fitness of FMDV in cytolytic infections. Even if not involved in the spreading of the virus in cytolytic infections (indicated by their normal plaque size) or thermostability (see above), residues Cys3007 and Met3014, alone or together with Asp3009, could be needed for some other step(s) of the virus life cycle, and this could lead to a reduction in biological fitness. To evaluate the fitness of the viable C3007V, M3014L, and D3009A/M3014L mutants relative to the nonmutated virus, we carried out competition assays between the latter virus and each of those mutants. Equal amounts of PFU of the two viruses to be competed were used to infect cells, and the procedure was cyclically repeated for up to eight passages. The progeny virus populations were sequenced, and the appropriate peaks in the chromatograms were integrated to obtain an approximate estimation of the relative abundance of the residue type at each position.

In the case of the M3014L mutant against the nonmutated virus, serial passaging of the virus mixture led to a gradual increase in the nonmutated genotype that was highly dominant from passage 6 onwards in two independent competition experiments (Fig. 3A). Sequencing of the entire capsid region of the resulting populations (passage 8) showed no mutation present in a detectable proportion at any position.

In the case of the D3009A/M3014L double mutant, contrary to what was observed for the M3014L single mutant, serial passaging of the virus mixture led to a sharp increase in the doubly mutated genotype, starting at passage 5, in two independent competition experiments (Fig. 3B.1). In addition, a new mutation, P1104T, emerged in the competing populations (Fig. 3B.2). However, in passage 6, the D3009A/M3014L mutation was nearly fully dominant, whereas the P1104T mutation was present in only 50% of the molecules and did not reach substantial dominance until later passages. Sequencing of the entire capsid region of the final population (passage 8) obtained in the two competition experiments showed that the

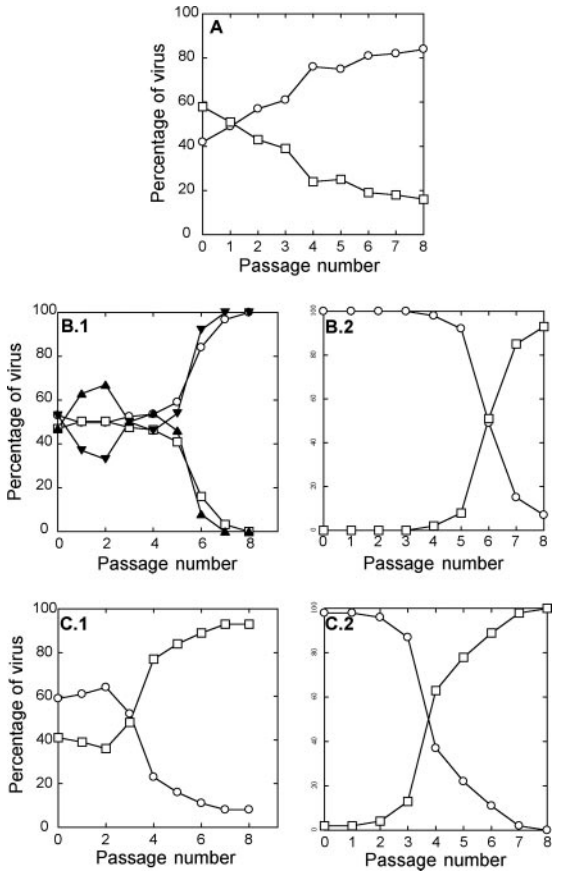

FIG. 3. Approximate percentage of FMDV genomes carrying a specific residue at a defined position during serial passages in competition experiments. The global sequence of the viral populations obtained after each passage was determined by automated sequencing, and the relative abundance of each residue type at the positions of interest was estimated from the ratio between the integrated areas of the corresponding bands in the chromatograms, as described in Materials and Methods. (A) Competition between the M3014L mutant and the parental virus. Circles, Met; squares, Leu at position 3014. (B) Competition between the D3009A/M3014L mutant and the parental virus. (B.1) Circles, Ala; squares, Asp at position 3009; black inverted triangles, Leu; black triangles, Met at position 3014. (B.2) Squares, Thr; circles, Pro at position 1104. (C) competition between the C3007V mutant and the parental virus. (C.1) Squares, Val; circles, Cys at position 3007. (C.2) Squares, Ala; circles, Asp at position 3009. All three competition assays were carried out in duplicate or triplicate with very similar results.

D3009A and M3014L mutations had reached full dominance and that P1104T was present in about 90% of the molecules.

The above-mentioned observations indicate that in cytolytic infections, the M3014L mutation is biologically disadvantageous and that D3009A causes strongly reduced viability when introduced in isolation; however, the introduction of D3009A leads to the fixation of M3014L. The two disadvantageous mutations together could yield a near neutral genotype relative to the nonmutated genotype, because the relative abundance of both viruses was not significantly altered during the first passages in competition assays. The final takeover by the mutant could have been caused exclusively by the fixation of an additional mutation, P1104T. However, the takeover and the fixation of this mutation were not concomitant (see above). We

consider it more likely that the 3009/3014 double mutation conferred a slight advantage that may have been potentiated by the effect of the P1104T mutation.

In the case of the C3007V mutant against the nonmutated virus, contrary to what could be expected from the high conservation of Cys3007 in viruses from acute infections, the nonmutated virus did not reach dominance. Instead, in three independent competition experiments, the proportion of viruses carrying the C3007V mutation increased from passage 3 upwards, and in the last passages, they had reached full dominance (Fig. 3C.1). Remarkably, in all three competitions, the D3009A mutation became gradually fixed in the population together with C3007V (Fig. 3C.2). The entire genome of the progeny virus at passage 8 of the three series was sequenced, and no other mutations in addition to C3007V and D3009A were found. Thus, the presence of Val instead of Cys at position 3007 is biologically not advantageous in cytolytic infections but allows the fixation of Ala instead of Asp at position 3009, leading to the dominance of the double mutant.

Finally, we investigated the functional reason why those virus variants with compensatory mutations, specifically C3007V/D3009A, may show increased biological fitness. The viral progeny yields obtained upon infection with this mutant, the C3007V single mutant, or the nonmutated virus were similar, as were their plaque sizes. However, infection kinetic assays showed that the double mutant produced extracellular progeny viruses significantly faster, reaching the maximum amount in about 8 h, while the C3007V mutant and the nonmutated control reached similar titers but only after 24 h (Fig. 4). This suggests that the increased fitness of the C3007V/D3009A mutant is due, at least in part, to a faster multiplication rate.

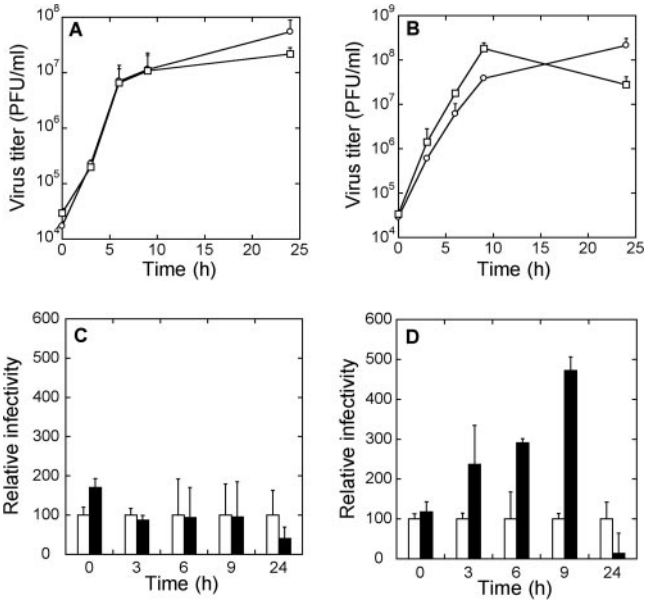

FIG. 4. Kinetics of extracellular virus production of nonmutated and mutant FMDVs. (A and B) Absolute virus titers at different times after infection. (A) Circles, nonmutated virus; squares, C3007V mutant. (B) Circles, nonmutated virus; squares, C3007V/D3009A mutant. (C and D) Relative infectivity of mutant viruses with respect to the infectivity of the nonmutated virus at different times after infection. The infectivity of the nonmutated virus at each time after infection has been given the reference value of 100. (C) White bars, nonmutated virus; black bars, C3007V mutant. (D) White bars, nonmutated virus; black bars, C3007V/D3009A mutant. Standard deviations are indicated in each case.

DISCUSSION

Is the cluster of mutations found around the fivefold axes in the FMDV R100 capsid a direct consequence of the modified environment during a persistent infection? It has been proposed that positions that are highly invariant in FMDV, or any other RNA virus, may readily change when viral replication occurs in a modified environment (16). More recent results (22, 49, 54) and those of the present study support the possibility that the modified environment during persistent infections could have led to the fixation of the D3009A mutation in the FMDV capsid. Of the four mutations detected around the fivefold axis pores in the capsid of FMDV R100, the D3009A mutation is the only one invariably found in FMDV populations rescued from cells that had been persistently infected (16, 22, 54; M. Herrera and E. Domingo, personal communication). The D3009A, N3013H, and M3014L (but not C3007V) mutations were also found in another population (R99) recovered from persistently infected cells (54). However, both R99 and R100 were obtained after just four or five further passages of a same cell population that had been split at a late passage. Although more complex mutation dynamics cannot be excluded, the simplest explanation for the presence of the D3009A, N3013H, and M3014L mutations in both R99 and R100 is that these mutations were fixed only once, before splitting at cell passage 95. On the other hand, D3009A (but not C3007V, N3013H, or M3014L) was repeatedly fixed in totally independent FMDV populations shed from persistently infected cells that had been cured from a FMDV infection and that were still partially resistant to viruses from lytic infections (22). Parallel infections of these cells with a type C FMDV isolate (different from C-S8c1) yielded progeny populations (C_3-Rb) that showed, like R100, modified phenotypic traits including increased virulence in normal BHK cells. In each of these populations, only two mutations became fixed in the capsid, D3009A and either G1110R or H1108R in VP1, with all three located very close to each other in the capsid structure. Complete sequencing of one of these populations showed that no other mutation had been fixed in the entire genome (22). In addition, of the four residues mutated around the capsid pores in FMDV R100, Asp3009 is the only one that is almost strictly conserved (98%) in the more than 200 sequences analyzed from isolates derived (in all probability) from acute/lytic infections. Furthermore, while the C3007V, N3013H, and M3014L mutations of R100 did not revert in the course of independent serial cytolytic passages of this virus, the D3009A mutation was not preserved in five out of the six serial infections analyzed. In these five cases, another residue (Thr) was fixed instead of Ala at position 3009 during replication of R100 in cytolytic infections (22). In brief, D3009A stands as the only mutation in R100 that (i) has been repeatedly observed in all FMDV populations rescued from cells that had been persistently infected, (ii) was not preserved when one of these populations was subjected to cytolytic infections, and (iii) was detected in only a few of the many FMDV isolates from acute/lytic infections that were analyzed. These observations are con-

sistent with the possibility that D3009A in the FMDV capsid may repeatedly arise as a consequence of the modified environment found in a persistent infection. This mutation was also found in about 2% of the FMDV sequences in the database. Most of these correspond to viral isolates that were probably derived from acute infections. As they are consensus sequences, they may not derive from viruses recovered from a small fraction of persistently infected cells in the host. Thus, the D3009A mutation may not be exclusive of persistent infections, and, if infrequent, it could also arise in response to other, unusual situations.

Unlike D3009A, other mutations fixed around the capsid pores in R100 (C3007V, N3013H, and M3014L) may have *not* occurred as a necessary consequence of a modified environment in persistently infected cells. These mutations were not fixed in other virus populations rescued from cells that had been persistently infected (22, 54). In addition, sequence analysis showed that Val or Leu was present at position 3007 or 3014 in as many as 11% or 54% of the more than 200 FMDV isolates from acute/lytic infections, respectively. His at position 3013 was not observed in viruses not related to persistent infections, but Asn at this latter position was not conserved either, as it was present in only 19% of the isolates. More importantly, in the present study, we showed that some of these mutations in R100 also became repeatedly fixed during cytolytic infections in response to the introduction of a previous mutation, as discussed below.

Linked mutational events may occur in response to the introduction of other mutations in the FMDV capsid. Our results also suggest that D3009A, irrespective of its role in a persistent infection, may be the key mutation for a series of linked mutational events in the FMDV capsid that involved a cluster of residues around the fivefold axis pores. The C3007V mutant outcompeted C-S8c1 but only through the fixation of the D3009A mutation. The D3009A mutant obtained by site-directed mutagenesis (mimicking the possible natural fixation of this mutation during a persistent infection) yielded high titers only through the fixation of the M3014L mutation. The introduction of the D3009A/M3014L double mutation facilitated the fixation of the N3013H mutation. Finally, the D3009A/M3014L mutation led, in competition experiments, to the fixation of a new mutation, P1104T, in a residue located close to the other mutated residues. In addition, every FMDV isolate analyzed that carried the D3009A mutation also carried an accompanying mutation of another residue that is spatially very close to residue 3009. These second mutations included C3007V or C3007A, S3008T or S3008A, N3013H, M3014L, and V3015Q in VP3 and H1108R, G1110R, and V1112L in VP1. Four of these mutations (S3008T, N3013H, H1108R, and G1110R) were very rarely observed in isolates that did not have the D3009A mutation, suggesting a linkage with D3009A. The introduction of a mutation like D3009A in a specific region of the virus capsid (either as a natural consequence of a modified environment, for example, during persistence, or by force using site-directed mutagenesis) may facilitate, or even require, the fixation of other mutations at neighboring locations.

Mutually compensatory effects of individually disadvantageous mutations may occur in the FMDV capsid. The results have shown that the D3009A and M3014L mutations are, per se, biologically disadvantageous and that C3007V may be slightly disadvantageous or, at least, does not provide a selective advantage. However, the simultaneous presence of D3009A and M3014L or of C3007V and D3009A led to an increase of the biological fitness relative to that of the nonmutated virus. The possibility of a putative substitution outside the capsid region in the viral RNA cannot be completely excluded in some instances. However, we consider this possibility to be unlikely. First, the same substitutions in the capsid repeatedly occurred in response to the same previous mutations; second, many compensating molecular events involve spatially close residues, as observed in our study; finally, in one case, the entire mutant genome was sequenced, and no other mutation was found. These observations provide clear evidence of second-site mutations that, even though intrinsically disadvantageous, may not only compensate for the detrimental effects of the primary mutations but also lead to the acquisition of new phenotypic characteristics that may provide a selective advantage. These effects open new possibilities for virus evolution.

An understanding of the structural basis of these compensatory effects must await further studies. However, note that the mutations fixed in response to other mutations (D3009A in response to C3007V, M3014L in response to D3009A, or N3013H in response to D3009A/M3014L) involved residues that are spatially in contact with or very close to each other, form a part of the interprotomer interfaces, and closely surround the pores at the capsid fivefold axes (Fig. 1). A likely possibility, which awaits testing, is that some of these compensation effects could be related to the kinetics of virion assembly. They could be also related to translocation events that might occur through permanent or transient capsid openings. Such translocation events have been detected in icosahedral viruses including picornaviruses. For example, in the minute virus of mice, a parvovirus, mutations of residues surrounding either the fivefold axis pores or buried cavities located close to the pores were shown to affect a conformational rearrangement associated with the translocation of the VP2 N terminus through the pores, an event that is needed for infectivity (9, 47). An impaired or untimely translocation event was also proposed to explain these effects (9). In coxsackievirus A9, a picornavirus, mutation of some residues at interprotomer interfaces located close to the capsid pores could result in the untimely or hindered externalization of the VP1 N terminus together with VP4 (2). In poliovirus, recent results indicate that the externalization of the myristoylated capsid protein VP4 and the N terminus of VP1, which are required for infectivity, takes place not through the fivefold axis pores but through transient openings at the interface between VP1 and VP3 that occur after a conformational change of the capsid (8). Further studies are required to determine whether the complex effect of mutations like C3007V, D3009A, and M3014L in the capsid of FMDV R100 could be related to a putative conformational rearrangement of the capsid and a translocation event, through either the pores or other transient openings, on the virion (under study).

To conclude, from the point of view of viral genetics, this study (i) indicates that the clustering of mutations at conserved residues around the fivefold axes in the capsid of an FMDV variant rescued from a persistent infection may also occur in cytolytic infections in response to changes in the local struc-

tural context, rather than being a direct consequence of adaptation to a different environment, and (ii) provides evidence for a chain of deterministic, mutually compensatory effects of individually disadvantageous or neutral mutations in the FMDV capsid that also led to the acquisition of new phenotypic traits.

ACKNOWLEDGMENTS

We gratefully acknowledge Esteban Domingo for critical reading of the manuscript and Celia Perales for help with some sequencing experiments.

This work was supported by grants from the Spanish Ministerio de Ciencia y Tecnología (BIO2003-04445 and BIO2006-00793) and Comunidad Autónoma de Madrid to M.G.M. and by an institutional grant from the Fundación Ramón Areces.

REFERENCES

1. **Acharya, R., E. Fry, D. Stuart, G. Fox, D. Rowlands, and F. Brown.** 1989. The three-dimensional structure of foot-and-mouth disease virus at 2.9 Å resolution. Nature **337:**709–716.
2. **Airaksinen, A., M. Roivainen, and T. Hovi.** 2001. Coxsackievirus A9 VP1 mutants with enhanced or hindered A particle formation and decreased infectivity. J. Virol. **75:**952–960.
3. **Almond, B. D., and D. H. Dean.** 1993. Suppression of protein structure destabilizing mutations in Bacillus thuringiensis delta-endotoxins by second site mutations. Biochemistry **32:**1040–1046.
4. **Baranowski, E., N. Sevilla, N. Verdaguer, C. M. Ruiz-Jarabo, E. Beck, and E. Domingo.** 1998. Multiple virulence determinants of foot-and-mouth disease virus in cell culture. J. Virol. **72:**6362–6372.
5. **Blacklow, S. C., and J. R. Knowles.** 1990. How can a catalytic lesion be offset? The energetics of two pseudorevertant triosephosphate isomerases. Biochemistry **29:**4099–4108.
6. **Bouvier, S. E., and A. R. Poteete.** 1996. Second-site reversion of a structural defect in bacteriophage T4 lysozyme. FASEB J. **10:**159–163.
7. **Brown, K. A., E. E. Howell, and J. Kraut.** 1993. Long-range structural effects in a second-site revertant of a mutant dihydrofolate reductase. Proc. Natl. Acad. Sci. USA **90:**11753–11756.
8. **Bubeck, D., D. J. Filman, N. Cheng, A. C. Steven, J. M. Hogle, and D. M. Belnap.** 2005. The structure of the poliovirus 135S cell entry intermediate at 10-angstrom resolution reveals the location of an externalized polypeptide that binds to membranes. J. Virol. **79:**7745–7755.
9. **Carreira, A., and M. G. Mateu.** 2006. Structural tolerance versus functional intolerance to mutation of hydrophobic core residues surrounding cavities in a parvovirus capsid. J. Mol. Biol. **360:**1081–1093.
10. **Chanel-Vos, C., and M. Kielian.** 2006. Second-site revertants of a Semliki Forest virus fusion-block mutation reveal the dynamics of a class II membrane fusion protein. J. Virol. **80:**6115–6122.
11. **Cimarelli, A., S. Sandin, S. Hoglund, and J. Luban.** 2000. Rescue of multiple viral functions by a second-site suppressor of a human immunodeficiency virus type 1 nucleocapsid mutation. J. Virol. **74:**4273–4283.
12. **Das, G., D. R. Hickey, D. McLendon, G. McLendon, and F. Sherman.** 1989. Dramatic thermostabilization of yeast iso-1-cytochrome c by an asparagine-isoleucine replacement at position 57. Proc. Natl. Acad. Sci. USA **86:**496–499.
13. **de la Torre, J. C., M. Dávila, F. Sobrino, J. Ortín, and E. Domingo.** 1985. Establishment of cell lines persistently infected with foot-and-mouth disease virus. Virology **145:**24–35.
14. **de la Torre, J. C., E. Martínez-Salas, J. Díez, A. Villaverde, F. Gebauer, E. Rocha, M. Dávila, and E. Domingo.** 1988. Coevolution of cells and viruses in a persistent infection of foot-and-mouth disease virus in cell culture. J. Virol. **62:**2050–2058.
15. **Deom, C. M., and X. Z. He.** 1997. Second-site reversion of a dysfunctional mutation in a conserved region of the tobacco mosaic tobamovirus movement protein. Virology **232:**13–18.
16. **Díez, J., M. Dávila, C. Escarmís, M. G. Mateu, J. Domínguez, J. J. Pérez, E. Giralt, J. A. Melero, and E. Domingo.** 1990. Unique amino acid substitutions in the capsid proteins of foot-and-mouth disease virus from a persistent infection in cell culture. J. Virol. **64:**5519–5528.
17. **Domingo, E., (ed.).** 2006. Current topics in microbiology and immunology, vol. 299. Quasispecies. Concepts and implications for virology. Springer, New York, NY. Curr. Top. Microbiol. Immunol. **299:**51–82.
18. **Domingo, E., and J. J. Holland.** 1997. RNA virus mutations and fitness for survival. Annu. Rev. Microbiol. **51:**151–178.
19. **Domingo, E., C. Escarmís, L. Menéndez-Arias, and J. J. Holland.** 1999. Viral quasispecies and fitness variations, p. 141–161. *In* E. Domingo, R. G. Webster, and J. J. Holland (ed.), Origin and evolution of viruses. Academic Press, San Diego, CA.
20. **Domingo, E., C. Biebricher, M. Eigen, and J. J. Holland.** 2001. Quasispecies and RNA virus evolution: principles and consequences. Landes Bioscience, Austin, TX.
21. **Ebert, C. E., and D. S. Beattie.** 2004. A compensatory double mutation of the alanine-86 to leucine mutant located in the hinge region of the iron-sulfur protein of the yeast cytochrome bc1 complex. Arch. Biochem. Biophys. **429:**16–22.
22. **Escarmís, C., E. C. Carrillo, M. Ferrer, J. F. García-Arriaza, N. López, C. Tami, N. Verdaguer, E. Domingo, and M. T. Franze-Fernández.** 1998. Rapid selection in modified BHK-21 cells of a foot-and-mouth disease virus variant showing alterations in cell tropism. J. Virol. **72:**10171–10179.
23. **Fares, M. A., and S. A. A. Travers.** 2006. A novel method for detecting intramolecular coevolution: adding a further dimension to selective constraints analysis. Genetics **173:**9–21.
24. **Filman, D. J., R. Syed, M. Chow, A. J. Macadam, P. D. Minor, and J. M. Hogle.** 1989. Structural factors that control conformational transitions and serotype specificity in type 3 poliovirus. EMBO J. **8:**1567–1579.
25. **Hartzog, P. E., and B. D. Cain.** 1994. Second-site suppressor mutations at glycine 218 and histidine 245 in the alpha subunit of F1F0 ATP synthase in Escherichia coli. J. Biol. Chem. **269:**32313–32317.
26. **Jarvik, J., and D. Botstein.** 1975. Conditional-lethal mutations that suppress genetic defects in morphogenesis by altering structural proteins. Proc. Natl. Acad. Sci. USA **72:**2738–2742.
27. **Joerger, A. C., M. D. Allen, and A. R. Fersht.** 2004. Crystal structure of a superstable mutant of human p53 core domain. Insights into the mechanism of rescuing oncogenic mutations. J. Biol. Chem. **279:**1291–1296.
28. **Kim, H.-W., T. J. Shen, D. P. Sun, N. T. Ho, M. Madrid, M. F. Tam, M. Zou, P. F. Cottam, and C. Ho.** 1994. Restoring allosterism with compensatory mutations in hemoglobin. Proc. Natl. Acad. Sci. USA **91:**11547–11551.
29. **Klig, L. S., D. L. Oxender, and C. Yanofsky.** 1988. Second-site revertants of Escherichia coli trp repressor mutants. Genetics **120:**651–655.
30. **Kondrashov, A. S., S. Sunyaev, and F. A. Kondrashov.** 2002. Dobzhansky-Muller incompatibilities in protein evolution. Proc. Natl. Acad. Sci. USA **99:**14878–14883.
31. **Kulathinal, R. J., B. R. Bettencourt, and D. L. Hartl.** 2004. Compensated deleterious mutations in insect genomes. Science **306:**1553–1554.
32. **Lea, S., J. Hernández, W. Blakemore, E. Brocchi, S. Curry, E. Domingo, E. Fry, R. Abu-Ghazaleh, A. King, J. Newman, D. Stuart, and M. G. Mateu.** 1994. The structure and antigenicity of a type C foot-and-mouth disease virus. Structure **2:**123–139.
33. **Machingo, Q., M. Mazourek, and W. Cameron.** 2001. Second-site, intragenic alterations in the gene encoding subunit II of cytochrome c oxidase from yeast can suppress two different missense mutations. Curr. Genet. **39:**297–304.
34. **Martín-Hernández, A. M., E. C. Carrillo, N. Sevilla, and E. Domingo.** 1994. Rapid cell variation can determine the establishment of a persistent viral infection. Proc. Natl. Acad. Sci. USA **91:**3705–3709.
35. **Mateo, R., A. Díaz, E. Baranowski, and M. G. Mateu.** 2003. Complete alanine scanning of intersubunit interfaces in a foot-and-mouth disease virus capsid reveals critical contributions of many side chains to particle stability and viral function. J. Biol. Chem. **278:**41019–41027.
36. **Mateu, M. G., and A. R. Fersht.** 1999. Mutually compensatory mutations during evolution of the tetramerization domain of tumor suppressor p53 lead to impaired hetero-oligomerization. Proc. Natl. Acad. Sci. USA **96:**3595–3599.
37. **Nikolova, P. V., K. B. Wong, B. DeDecker, J. Henckel, and A. R. Fersht.** 2000. Mechanism of rescue of common p53 cancer mutations by second-site suppressor mutations. EMBO J. **19:**370–378.
38. **Nijhuis, M., R. Schuurman, D. de Jong, J. Erickson, E. Gustchina, J. Albert, P. Schipper, S. Gulnik, and C. A. Boucher.** 1999. Increased fitness of drug-resistant HIV-1 protease as a result of acquisition of compensatory mutations during suboptimal therapy. AIDS **13:**2349–2359.
39. **Olivares, I., V. Sánchez-Merino, M. A. Martínez, E. Domingo, C. López-Galíndez, and L. Menéndez-Arias.** 1999. Second-site reversion of a human immunodeficiency virus type 1 reverse transcriptase mutant that restores enzyme function and replication capacity. J. Virol. **73:**6293–6298.
40. **Olivares, I., M. Gutiérrez-Rivas, C. López-Galíndez, and L. Menéndez-Arias.** 2004. Tryptophan scanning mutagenesis of aromatic residues within the polymerase domain of HIV-1 reverse transcriptase: critical role of Phe-130 for p51 function and second-site revertant restoring viral replication capacity. Virology **324:**400–411.
41. **Ono, A., M. Huang, and E. O. Freed.** 1997. Characterization of human immunodeficiency virus type 1 matrix revertants: effects on virus assembly, Gag processing, and Env incorporation into virions. J. Virol. **71:**4409–4418.
42. **Pazhanisamy, S., C. M. Stuver, A. B. Cullinan, N. Margolin, B. G. Rao, and D. J. Livingston.** 1996. Kinetic characterization of human immunodeficiency virus type-1 protease-resistant variants. J. Biol. Chem. **271:**17979–17985.
43. **Pelemans, H., R. Esnouf, K. L. Min, M. Parniak, E. De Clercq, and J. Balzarini.** 2001. Mutations at amino acid positions 63, 189, and 396 of human immunodeficiency virus type 1 reverse transcriptase (RT) partially restore the DNA polymerase activity of a Trp229Tyr mutant RT. Virology **287:**143–150.

44. **Poon, A., and L. Chao.** 2005. The rate of compensatory mutation in the DNA bacteriophage ΦX174. Genetics **170:**989–999.
45. **Poteete, A. R., D. Rennell, S. E. Bouvier, and L. W. Hardy.** 1997. Alteration of T4 lysozyme structure by second-site reversion of deleterious mutations. Protein Sci. **6:**2418–2425.
46. **Regan, L., L. Buxbaum, K. Hill, and P. Schimmel.** 1988. Rationale for engineering an enzyme by introducing a mutation that compensates for a deletion. J. Biol. Chem. **263:**18598–18600.
47. **Reguera, J., A. Carreira, L. Riolobos, J. M. Almendral, and M. G. Mateu.** 2004. Role of interfacial amino acid residues in assembly, stability and conformation of a spherical virus capsid. Proc. Natl. Acad. Sci. USA **101:** 2724–2729.
48. **Sapunaric, F. M., and S. B. Levy.** 2003. Second-site suppressor mutations for the serine 202 to phenylalanine substitution within the interdomain loop of the tetracycline efflux protein Tet(C). J. Biol. Chem. **278:**28588–28592.
49. **Sevilla, N., and E. Domingo.** 1996. Evolution of a persistent aphthovirus in cytolytic infections: partial reversion of phenotypic traits accompanied by genetic diversification. J. Virol. **70:**6617–6624.
50. **Shiomi, H., T. Urasawa, S. Urasawa, N. Kobayashi, S. Abe, and K. Taniguchi.** 2004. Isolation and characterization of poliovirus mutants resistant to heating at 50°C for 30 min. J. Med. Virol. **74:**484–491.
51. **Sobrino, F., M. Dávila, J. Ortín, and E. Domingo.** 1983. Multiple genetic variants arise in the course of replication of foot-and-mouth disease virus. Virology **128:**310–318.
52. **Tachedjian, G., H. E. Aronson, and S. P. Goff.** 2000. Analysis of mutations and suppressors affecting interactions between the subunits of the HIV type 1 reverse transcriptase. Proc. Natl. Acad. Sci. USA **97:**6334–6339.
53. **Thompson, J. R., S. Doun, and K. L. Perry.** 2006. Compensatory capsid protein mutations in cucumber mosaic virus confer systematic infectivity in squash (*Cucurbita pepo*). J. Virol. **80:**7740–7743.
54. **Toja, M., C. Escarmís, and E. Domingo.** 1999. Genomic nucleotide sequence of a foot-and-mouth disease virus clone and its persistent derivatives. Implications for the evolution of viral quasispecies during a persistent infection. Virus Res. **64:**161–171.
55. **Twomey, T., L. L. France, S. Hassard, T. G. Burrage, J. F. E. Newman, and F. Brown.** 1995. Characterization of an acid-resistant mutant of foot-and-mouth disease virus. Virology **206:**69–75.
56. **Wray, J. W., W. A. Baase, J. D. Lindstrom, L. H. Weaver, A. R. Poteete, and B. W. Matthews.** 1999. Structural analysis of a non-contiguous second-site revertant in T4 lysozyme show that increasing the rigidity of a protein can enhance its stability. J. Mol. Biol. **292:**1111–1120.
57. **Wu, T. D., C. A. Schiffer, M. J. Gonzales, J. Taylor, R. Kantor, S. Chou, D. Israelski, A. R. Zolopa, W. F. Fessel, and R. W. Shafer.** 2003. Mutation patterns and structural correlates in human immunodeficiency virus type 1 protease following different protease inhibitor treatments. J. Virol. **77:**4836–4847.
58. **Yamaguchi, A., R. O'vauchi, Y. Someva, T. Akasaka, and T. Sawai.** 1993. Second-site mutation of Ala-220 to Glu or Asp suppresses the mutation of Asp-285 to Asn in the transposon Tn10-encoded metal tetracycline/H^+ antiporter of Escherichia coli. J. Biol. Chem. **268:**26990–26995.
59. **Yuan, T. T., and C. Shih.** 2000. A frequent, naturally occurring mutation (P130T) of human hepatitis B virus core antigen is compensatory for immature secretion phenotype of another frequent variant (I97L). J. Virol. **74:** 4929–4932.
60. **Zibert, A., G. Maass, K. Strebel, M. M. Falk, and E. Beck.** 1990. Infectious foot-and-mouth disease virus derived from a cloned full-length cDNA. J. Virol. **64:**2467–2473.